Flow Measurement and Instrumentation 79 (2021) 101951

Contents lists available at ScienceDirect

Flow Measurement and Instrumentation

journal homepage: www.elsevier.com/locate/flowmeasinst

Investigating reproducibility in multiphase flow metrology: Results from an intercomparison of laboratories

A.J. Elliott [a,*], G. Falcone [a], D. van Putten [b], T. Leonard [c], K. Haukalid [d], B. Pinguet [c]

[a] James Watt School of Engineering, University of Glasgow, Glasgow, G12 8QQ, UK
[b] DNV GL, Groningen, Netherlands
[c] TÜV SÜD National Engineering Laboratory (NEL), Glasgow, UK
[d] NORCE, Bergen, Norway

ARTICLE INFO

Keywords:
Multiphase flow
Metrology
Laboratory intercomparison

ABSTRACT

This paper presents the results of an intercomparison of multiphase flow laboratories. Conducted as part of EMPIR project *16ENG07 – MultiFlowMet II*, the primary focus of the investigation was to determine the influence of laboratory-specific factors on the reproducibility of measurements made by multiphase flow metres (MPFMs). To minimise these effects as much as possible, a portable transfer package was designed, including the MPFM, a transparent viewing section, and a straight pipe section with a length of 100 internal pipe diameters. A reproducibility parameter, ζ, was developed to quantify both the reproducibility of the transfer package. Across the three laboratories, metrological compatibility was achieved for the majority of test points. By presenting the ζ values as functions of the gas volume fraction (GVF) and water liquid ratio (WLR), it was possible to identify flow regimes that may be more susceptible to reductions in reproducibility.

1. Introduction

While the global energy industry continues to make important steps towards carbon neutral production, traditional oil and gas fuels still have an important role to play in meeting energy demands and ensuring a smooth transition over the coming decades. To ensure that individual energy security is not sacrificed, it is becoming increasingly necessary to utilise complex oil and gas fields, such as subsea resources. Accurate multiphase flow metrology is vital in enabling these resources to be utilised in a safe and sustainable manner. However, field measurements of multiphase flow typically have a high degree of uncertainty (up to 20% in some conditions [1]), so it is necessary to develop reference measurement capabilities that are consistent and comparable across different multiphase flow laboratories.

To address this need for reproducible multiphase flow metrology, the EMPIR project *16ENG07 – MultiFlowMet II* [1] was established. This project expands the original EMRP project*ENG58 – MultiFlowMet*, that developed and piloted an approach to harmonise the metrology of multiphase flow. The results and findings of this project can be found in its Final Publishable JRP Report with Associated Annex [2], as well as in [3]. A key aim of both projects was to investigate the reproducibility of multiphase flow metres (MPFMs) between laboratories. To this end, a transfer package was designed to limit the impact of geometrical variances between the laboratories, as far as possible. However, it must be noted that it was not possible to harmonise some of the geometrical factors, such as fluid inlet positions, mixing distances, gas composition, and pressure. Further experimental studies were carried out to better understand the impact of these geometrical variances, with largely reassuring results. However, a detailed discussion of these variations is beyond the scope of the present intercomparison.

The transfer package was designed to be compliant with three leading multiphase flow laboratories. Namely, these were NEL in the UK, DNV GL in the Netherlands, and NORCE in Norway. A test matrix was defined across a range of liquid volumetric flow rates (Q_{liquid}), gas volume fractions (GVF) and water-in-liquid ratios (WLR) within the operating envelopes of the transfer metre and the participating laboratories. By varying the operating pressures and temperatures of the aforementioned laboratories, it was possible to match the flow parameters using dimensionless numbers.

2. Test protocol

As discussed above, the intercomparison study took place across three leading multiphase flow facilities; namely, NEL in the UK, DNV GL in the Netherlands, and NORCE in Norway. The study was divided into two similar comparisons: one at lower pressure, between NEL and NORCE, and one at higher pressure, between NEL and DNV GL. At each

* Corresponding author.
E-mail addresses: Alexander.Elliott@glasgow.ac.uk (A.J. Elliott), Gioia.Falcone@glasgow.ac.uk (G. Falcone).

https://doi.org/10.1016/j.flowmeasinst.2021.101951
Received 10 November 2020; Received in revised form 15 March 2021; Accepted 20 April 2021
Available online 24 April 2021

Nomenclature

Notation	Definition
$u(\bullet)$	Uncertainty in the measurement of $\bullet$
WLR	Water liquid ratio
GVF	Gas volume fraction
MPFM	Multiphase flow metre
U_{repro}	Reproducibility uncertainty
M	Generic measured variable
s	Standard variation
h	Mandel's h statistic
N_M	Total number of test points
Q	Volumetric flow rate

of these facilities, best efforts were made to maintain consistency across the test campaign, as will be outlined in this section.

A key motivation for this study was to assess the reproducibility of measurements between laboratories. In particular, despite the aforementioned efforts made, differences in flow loop design and fluid properties may influence flow patterns and metrology. A summary of these differences is presented in Table 1.

2.1. Operating conditions

Ideally, the comparison would be performed under exactly the same conditions at all laboratories. However, variations in operating ranges, different test fluids, and different geometrical configurations mean that this is not always possible. To account for the differences in test fluids and facility operating ranges, optimal facility operating conditions, including temperatures, pressures, and water salinity, were determined to achieve the best match of two key dimensionless numbers: the Froude number and oil Reynolds number. The Reynolds number gives the ratio of inertial and viscous forces. The Froude number gives the ratio of inertial and gravitational forces.

The densiometric Froude number for the gas and liquid phase are defined as [4]

$$\mathrm{Fr}_g = \frac{v_g}{\sqrt{gD}}\sqrt{\frac{\rho_g}{\rho_l - \rho_g}}, \tag{1}$$

$$\mathrm{Fr}_l = \frac{v_l}{\sqrt{gD}}\sqrt{\frac{\rho_l}{\rho_l - \rho_g}}, \tag{2}$$

where the subscripts $_g$ and $_l$ represent the gas and liquid phases, respectively, ρ denotes the density (kg/m^3), g is the acceleration due to gravity (m/s^2), v refers to the superficial phase velocity (m/s), and D is the internal diameter of the pipe.

It is possible to modify the following parameters to achieve the best match of Froude and Reynolds numbers:

- oil density and viscosity (via temperature),
- water density and viscosity (via temperature and salinity),
- gas density and viscosity (via temperature and pressure).

The optimal operating pressures and temperatures chosen for each laboratory to achieve the best match of Froude and Reynolds numbers are summarised in Table 2.

2.2. Transfer package

To maximise consistency between the three laboratories, a portable transfer package was designed. It includes the MPFM, discussed below, a transparent viewing section, and a straight pipe upstream of the transparent section, with a length of 100 internal pipe diameters (D).

Given that there are a number of differences in the system geometries, achieving consistency between laboratories and test conditions represents a key challenge. It must be noted that this holds true both for the laboratories included in the present study and in more general comparisons between facilities. The transfer package has been designed with this discussion in mind, and a 100D horizontal pipe has been included to minimise the effect of upstream variations.

The MPFM is based on the principle of gamma ray attenuation as the flow passes through a Venturi tube. Thus, the MPFM consists of three main sections:

- An impedance section, which has a 2–6 electrode geometry; here, signals are processed by impedance field electronics.
- A gamma densitometer, consisting of a detector and a Caesium-137 source.
- A Venturi section, consisting of a Venturi insert (with a beta ratio of 0.6), and a block and bleed valve providing dP, P, and T measurements via a multi-variable transmitter.

The MPFM measures the fraction of each phase through a combination of the impedance measurements and gamma attenuation. The Venturi, combined with cross-correlation in the impedance section, is used to provide the respective velocities. Once fluid properties are provided, the total flow rate of each phase can be calculated at both actual and standard conditions. To match the MPFM internal diameter of 67 mm, all pipe spools, viewing sections and tomography sensors forming the components of the transfer package were manufactured in 3-inch Schedule 160.

In addition to the MPFM, four separate tomography devices were installed along the 100D upstream pipe section. These were a University of Coventry Atout ECT sensor, two pipe spools containing the ITOMS ECT and ERT modules and a University of Bergen tomography unit. Where tomography sensors were not deployed at a particular test site, the sensors were replaced by spool pieces of matching dimensions in order to maintain the transfer package length and pipe internal diameter across the participating laboratories.

2.3. Test matrix

The initial test period performed during NEL Round 1 aimed to follow the test matrices given in Table 3. Naturally, there were some deviations from the values in the actual set points achieved and those listed in Table 3. To ensure an accurate comparison with the other test campaigns, the actual values achieved during NEL Round 1 were used to define the subsequent test matrices, rather than the exact values in Table 3.

3. Analysis methods

To ensure a fair and accurate inter-laboratory comparison, the statistical methodology applied to the data was performed in accordance with international standard ISO 5275-2:2019 [5]. This section will outline the statistical analysis applied to the data, including the determination and removal of unusable test points, as well as defining the uncertainty and reproducibility calculations.

3.1. Test point logging

A rigorous approach was taken to ensure consistency in the stability of the flow at each laboratory. This was achieved through the following steps:

1. The facility operator set up each test point, as defined in the test matrices, and provided confirmation when stabilised conditions had been reached.
2. The independent arbiter then monitored conditions at the MPFM location until stable, before giving approval to start logging the test point.

Table 1
Overview of the differences between multiphase flow laboratories participating in the intercomparison. The mixing distance represents the length of pipeline between the final inlet point and the start of the transfer package (*).

Characteristic	NEL, low press.	NEL, high press.	NORCE	DNV GL
Flow loop design	Open loop	Open loop	Closed loop	Closed loop
Injection type	Gas into liquid	Gas into liquid	Gas into liquid	Liquid into gas
Mixing distance* (m)	0	0	4	5–10
Oil viscosity (cP)	7.26 to 8.26	6.95 to 8.51	2.4 to 2.7	4.8 to 5.2
Gas density (kg/m^3)	5.54 to 6.41	9.74 to 11.21	6.26 to 7.47	8.52 to 12.03
Water density (kg/m^3)	1023.65 to 1025.49	1022.79 to 1025.89	1031.58 to 1032.07	1030.87 to 1032.03
Oil density (kg/m^3)	814.56 to 829.60	813.91 to 818.15	823.52 to 824.78	825.47 to 828.50

Table 2
Selected operating parameters and nominal fluid properties to best match dimensionless numbers between facilities.

Flow Lab.	Pressure (barg)	Temp (°C)	Water				Oil		
			Type	Salinity (wt.%)	Density (kg/m^3)	Viscosity (cP)	Type	Density (kg/m^3)	Viscosity (cP)
NEL	4.5	45	NaCl	4.8	1024.19	0.65	Paraflex HT9	814.81	7.32
NEL	9	45	NaCl	4.8	1024.19	0.65	Paraflex HT9	815.10	7.32
NORCE	4.5	25	NaCl	4.8	1031.99	0.99	Diesel	824.05	2.52
DNV GL	8	18	NaCl	4.8	1031.69	1.04	Exxsol D120	827.55	5.10

Table 3
Low and high pressure intercomparison test matrices.

Low pressure:								High pressure:							
Liquid flow rate (m^3/h)	Gas volume fraction (%)							Liquid flow rate (m^3/h)	Gas volume fraction (%)						
	10	30	50	67	80	90	95		10	30	50	67	80	90	95
5							X	5							X
15					X	X		15					X	X	
30			X	X	X			30			X	X	X		
50		X	X	X				50		X	X	X			
75	X	X						75	X	X	X	X			
100								100	X	X					

3. The facility operators, as well as any remote operators, commenced the log when the arbiter confirmed the test point was stable. The logging of the facility reference and MPFM measurements commenced simultaneously for a 10 min log duration.

The independent arbiter maintained an independent test log throughout the test campaigns documenting any notable observations.

3.2. Confirmation of useable test points

To ensure the fairness of all comparison test points, it was necessary to ensure a level of consistency between the flow rates achieved at each facility. The Mandel's h statistics have been used to assess whether any test points should be removed, as recommended in ISO 5275-2:2019 [5].

3.2.1. Mandel's h statistics

For inter-laboratory comparisons, ISO 5275-2:2019 [5] recommends the use of Mandel's h statistics to assess the consistency and variability of the results of each test campaign. This statistic was originally defined in [6] and the critical value, h_{crit}, has been formally defined in [7]. The process of calculating these values is briefly outlined here.

In general, the discussions presented in this work will denote a generic measurement (of volumetric flow, GVF, WLR) simply by the notation M. Further, to simplify the notation, each test campaign will be assigned an integer value from 1 to p. Therefore, the set $\{M_{i,1}, \dots, M_{i,p}\}$ will denote the measured values for a specific test point, TPi, with the second subscript representing the number of the laboratory in question. The mean value for each test point can be written as

$$\bar{M}_i = \frac{\sum_{j=1}^{p} M_{i,j}}{p}. \tag{3}$$

Then, the standard deviation, s_i, of the comparison for test point i can be calculated as

$$s_i = \sqrt{\frac{\sum_{j=1}^{p} d_{j,i}^2}{p-1}}, \tag{4}$$

where $d_{i,j} = M_{i,j} - \bar{M}_i$ is the deviation of lab j from the mean value of some measurement M_i.

The h value for lab j can then be calculated as

$$h_{i,j} = \frac{d_{i,j}}{s_i}. \tag{5}$$

To assess whether a test point should be removed from the statistical investigation, it is necessary to compare each $h_{i,j}$ to the critical h value, $h_{i,\text{crit}}$, calculated as [7]

$$h_{i,\text{crit}} = \frac{(p-1)t_{p-2;1-\alpha/2}}{\sqrt{p(p-2+t^2_{p-2;1-\alpha/2})}}. \tag{6}$$

where $t_{p-2;1-\alpha/2}$ is the $(1-\alpha/2)$-quantile of the Student's t-distribution, with $\nu = p-2$ degrees of freedom and significance level $\alpha = 0.05$. The values of $h_{i,j}$ are compared with $h_{i,\text{crit}}$ for the 4.5 barg and 9 barg comparisons in Figs. 1 and 2, respectively.

In Figs. 1 and 2, it can be observed that none of the h values exceed h_{crit}. Thus, it is reasonable to proceed with all test points included.

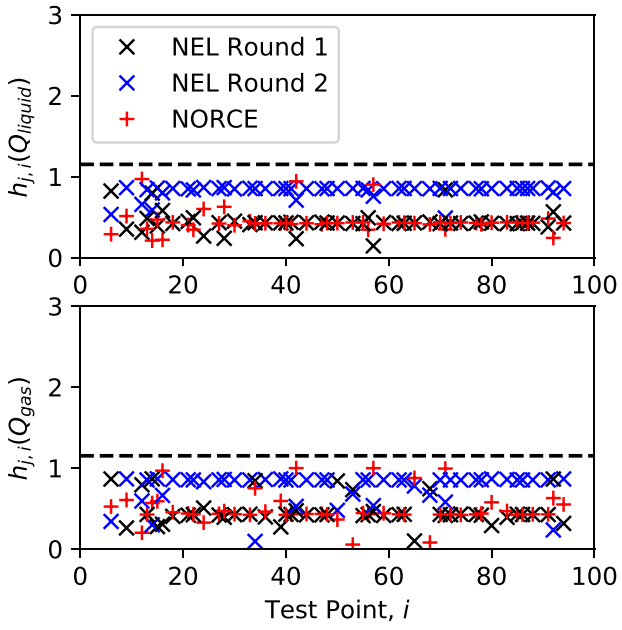

Fig. 1. Comparison of the h values associated for the flow rates achieved at 4.5 barg. The horizontal dashed line denotes the critical value h_{crit}.

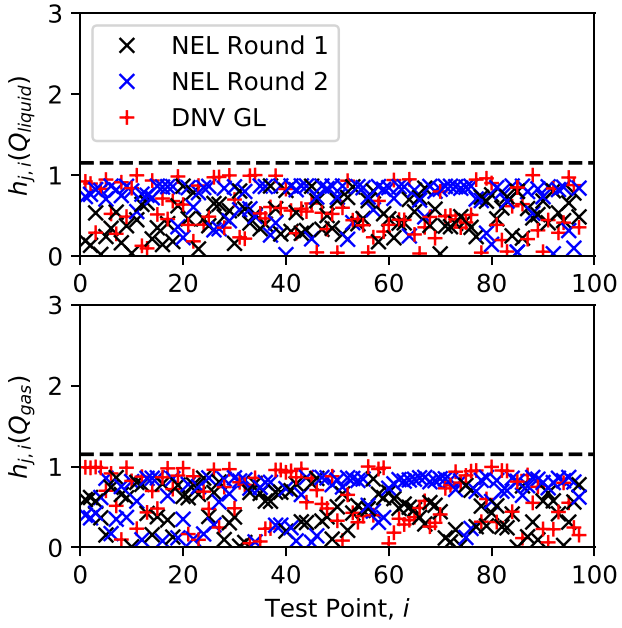

Fig. 2. Comparison of the h values associated for the flow rates achieved at 9 barg. The horizontal dashed line denotes the critical value h_{crit}.

3.3. Laboratory uncertainty variations

Although the previous section provides confirmation of the comparable test points, it must be noted that there are differences in the uncertainty of the measurements made at each laboratory. This is particularly important for the following sections, in which comparisons between differences in the measured flow rates and the uncertainty of the measurements are used to investigate metrological compatibility. To provide context for the discussion below, the average uncertainties for measurement of the single-phase liquid flow at each laboratory are provided in Table 4; note that the laboratory measurement system can allow for the uncertainties to be calculated for the individual liquids (oil and water) or the combined liquid phase, as is presented in Table 4.

The first row highlights one of the differences in the uncertainty approach between laboratories. In particular, the influence of phase transition between the inlet and test location may be incorporated into the calculation, and it is believed that the uncertainty associated is significant for some test points; further investigation into this phenomenon is beyond the scope of the present study, but will form the basis of a future investigation.

4. Transfer package reproducibility

A key aim of this work was to investigate the reproducibility of the transfer package. In this section, this is investigated through the calculation of the reproducibility uncertainties and through the use of a metrological compatibility parameter.

4.1. Reproducibility uncertainty

The reproducibility uncertainty is calculated using data from NEL Rounds 1 and 2. For each measured parameter, M, the number of acceptable test points included in the reproducibility calculation will be denoted N_M. Then, the reproducibility uncertainty of the MPFM for parameter M, denoted $u(M^{\mathrm{MPFM}})$, is calculated as the pooled standard deviation of N_M independent deviations:

$$u(M^{\mathrm{MPFM}}) = \sqrt{\frac{1}{N_M}\sum_{i=1}^{N_M}\left(\frac{M_{i,j_1} - M_{i,j_2}}{\sqrt{2}}\right)^2}. \tag{7}$$

From Eq. (7), it is possible to calculate the expanded reproducibility uncertainty, denoted U_{repro}. Assuming that the uncertainty follows a Normal distribution, a coverage factor of 2 can be used to define an interval having a confidence level of approximately 95%. A second factor of $\sqrt{2}$ is also included to account for the uncertainty of both measurements made by the MPFM. Thus, the expanded reproducibility uncertainty can be expressed as

$$U_{\mathrm{repro}} = 2\sqrt{2}u(M^{\mathrm{MPFM}}) \tag{8}$$

The calculated values for U_{repro} are presented in Table 5. These values are comparable with the corresponding uncertainties from the initial *MultiFlowMet* project [3], particularly for the fluid flow rates (liquid: 2.4%, water: 3.4%, oil: 5.6%), which observed smaller uncertainty in the low pressure results of the present work. However, the gas volume flow rate uncertainties are higher, leading to a similar trend in the total mass flow rate. The reason for this discrepancy is explored in the following section.

4.2. Pairwise metrological compatibility

To assess the reproducibility more thoroughly, the ζ reproducibility parameter defined in MultiFlowMet [2] was used to compare the flow conditions for each test point directly. This parameter is derived based on the ζ and E_n parameters defined in ISO 13528:2015 [8], as well as the supporting discussion in [9]. The discussions and figures regarding metrological compatibility in [9] are applied here to define ζ. First, a more general overview of the derivation of this parameter is provided, so that it may also be used for inter-laboratory comparisons in Section 5.

4.2.1. Defining the reproducibility parameter, ζ

In the current intercomparison, the *measurand* (i.e. the true value that should be captured by the metre) is the volumetric flow rate. For a given test point, i, and laboratory/test campaign, j, the volumetric flow rate is measured by the laboratory itself, denoted $Q_{i,j}$. Based on the Mandel's h test applied in Section 3.2, it is possible to follow the assumption presented in [2] that the reference measurements will be consistent between the labs, so that $Q_{i,\mathrm{ref}} = Q_{i,j_1} = Q_{i,j_2}$ for any pair of labs, j_1 and j_2. The uncertainty associated with the measurand is

Table 4
Physical and statistical characteristics achieved at each facility; these values were taken from the in-house measurements of each laboratory.

Parameter	NEL (low)	NEL (high)	NORCE	DNV GL
Phase transitions included?	No	No	Yes	Yes
$\bar{u}(Q_{\text{liquid}})$	0.41%	0.40%	0.21%	0.31%*
$\bar{u}$(WLR)	0.19 abs-%	0.18 abs-%	0.53 abs-%	0.11 abs-%*
$\bar{u}$(GVF)	0.12 abs-%	0.12 abs-%	0.38 abs-%	0.17 abs-%*

Starred (*) uncertainties are not calculated directly at DNV GL, so are calculated from the single-phase flow rate uncertainties.

Table 5
U_{repro} values for the measured parameters.

Quantity measured, M	U_{repro}, low pressure	U_{repro}, high pressure
Total volume flow rate, Q_{total}	6.3%	9.8%
Gas volume flow rate, Q_{gas}	5.7%	8.7%
Liquid volume flow rate, Q_{liquid}	1.9%	2.5%
Water volume flow rate, Q_{water}	1.4%	1.6%
Oil volume flow rate, Q_{oil}	1.4%	2.0%
Gas volume fraction, GVF	2.1 abs-%	2.3 abs-%
Water liquid ratio, WLR	5.1 abs-%	4.0 abs-%

assumed to be the uncertainty of the reference metre at each laboratory, denoted $u_{\text{ref},j} = u(Q_{i,j})$. Note that the subscript j is necessary due to the fact that the metre used to measure this reference flow rate varies between laboratories and test campaigns.

The *measurement* of this flow rate is then made by the MPFM, and denoted $Q_{i,j}^{\text{MPFM}}$. The uncertainty associated with this measurement arises solely from the uncertainty of the MPFM, which will be denoted $u_{\text{MPFM},j} = u(Q_{i,j}^{\text{MPFM}})$, and is provided by the manufacturer.

Finally, the *observation* of this measurement will be taken to mean the calculation of the relative deviation of the measurement of the measurand. This can be calculated as

$$\Delta Q_j = \frac{Q_{i,j} - Q_{i,j}^{\text{MPFM}}}{|Q_{i,j}|}. \tag{9}$$

Note that the relative deviation is selected instead of the absolute deviation, so that the results are not skewed at higher flow rates.

Where multiple observations are made, the mean will be taken, denoted $\overline{\Delta Q_j}$. The uncertainty associated with this deviation is denoted $\sigma(\Delta Q_j)$, and must account for the uncertainties of both the measurand and the measurement. Thus, it can be calculated as

$$\sigma(\Delta Q_j) = \sqrt{u_{\text{ref},j}^2 + u_{\text{MPFM},j}^2}. \tag{10}$$

Note that the current formulation is developed with the assumption that the correlation coefficient between the reference and MPFM measurements is 0.

Now that the appropriate statistical quantities have been defined, it is possible to create a ζ-function that can be used to assess the metrological compatibility of two particular results. The general form of a ζ-function is written as

$$\zeta(\Delta) = \frac{\Delta}{u(\Delta)}, \tag{11}$$

where Δ is some difference. In the present study, this is the difference between two deviations, which leads to the ζ reproducibility parameter proposed in [2]:

$$\pm\zeta_Q = \frac{\overline{\Delta Q_{j_1}} - \overline{\Delta Q_{j_2}}}{\sqrt{\sigma(\Delta Q_{j_1})^2 + \sigma(\Delta Q_{j_2})^2}}. \tag{12}$$

It can be noted that, since the reference flow rate is assumed to be the same at both laboratories, the numerator is effectively equal to $\overline{Q_{j_1}} - \overline{Q_{j_2}}$. The two measurements are metrologically compatible if $|\zeta| \leq \kappa$, for a particular threshold κ. In the present case, it is the standard uncertainties that are used, as opposed to the expanded uncertainties, so a value of $\kappa = 2$ is used. In similar calculations made in the initial *MultiFlowMet* project [3], it was the expanded uncertainties that were used, so a value of $\kappa = 1$ was used. Therefore, it can be concluded that the two measurements are compatible if the difference in observations is smaller than the combined uncertainties in their measurement.

The expanded interpretation of the ζ_Q value from MultiFlowMet is outlined in Table 6.

4.2.2. Pairwise reproducibility

The ζ parameter can now be used to give initial insight into the reproducibility of the transfer package. Throughout Figs. 3–16, the threshold value of $\kappa = \pm 2$ is represented by the horizontal, grey line.

The solid, blue and dashed, red lines denote the oil/water continuous inversion point for the first and second rounds of testing at NEL, respectively. These have been calculated using the binary indicator provided by the MPFM; this value has been multiplied by the WLR for each point and the average of these values has been calculated. It can immediately be observed that there is strong consistency between these values at both pressure levels.

Prior to discussion of trends in the reproducibility parameter values, it is important to highlight two test points, TP55 and TP56, that were shown to be transitioning from oil continuous to water continuous. This has potential implications for the reproducibility calculations, as the use of different MPFM modes would result in a comparison of two measurements that are inherently different. Particular attention is given to these points: TP55 and TP56 have been highlighted throughout this section with a green circle and magenta square, respectively.

The reproducibility of Q_{gas} is investigated in Figs. 3–6; it can be recalled, from Table 5, that the volumetric gas flow rate exhibited the highest values for U_{repro}, particularly at higher pressure. This is in line with the higher ζ_{gas} values observed in Figs. 5 and 6. For both pressures, the reproducibility parameters calculated are typically larger for higher WLRs, though metrological compatibility is achieved for all points. For the higher-pressure comparison (Figs. 5 and 6), the ζ_{gas} values are noticeably higher for the low-GVF points. A similar trend can be observed for the lower-pressure comparison, though this is less pronounced.

From Figs. 7–10, it is immediately clear that the $|\zeta_{liquid}|$ values are significantly lower than the corresponding gas flow rate reproducibility values. Once more, metrological compatibility was exhibited for the majority of test points at high pressure, and for all points at low pressure.

Although TP55 continues to show good reproducibility, at both pressures, TP56 shows a much greater deviation at higher pressure. As can be observed in Fig. 10, this TP falls almost exactly on the phase transition, highlighting the challenges of achieving reproducible measurements in this region.

The ζ_{water} trends, presented in Figs. 11–14, provide further insight into the test points with low reproducibility for the liquid volumetric

Table 6
Interpretation of the value of the ζ_O reproducibility parameter.

ζ value	Interpretation
$\lvert\zeta\rvert = 0$	Idealised case in which both laboratories achieve identical flow conditions and the MPFM exhibits perfect reproducibility.
$0 < \lvert\zeta\rvert \leq 2$	Strong statistical agreement between the measurements taken in the two test campaigns; metrological compatibility has been achieved.
$2 < \lvert\zeta\rvert \leq 3$	Doubtful reproducibility, further investigation required.
$\lvert\zeta\rvert > 3$	Comparison failed.

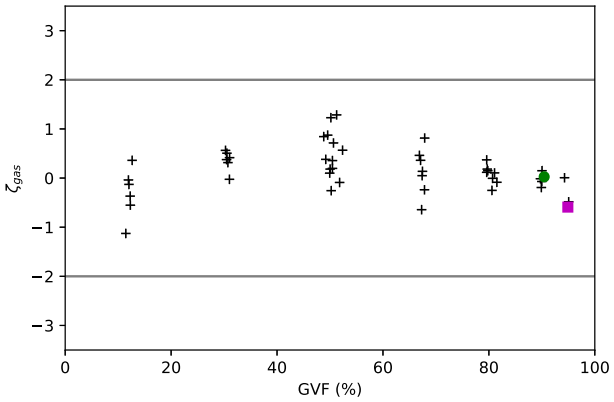

Fig. 3. Low pressure ζ_{gas} values presented as a function of GVF.

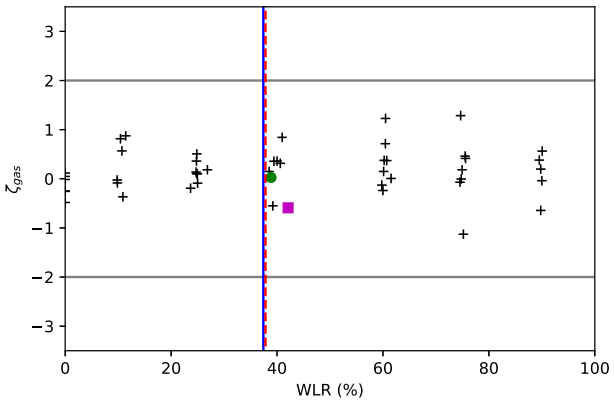

Fig. 4. Low pressure ζ_{gas} values presented as a function of WLR.

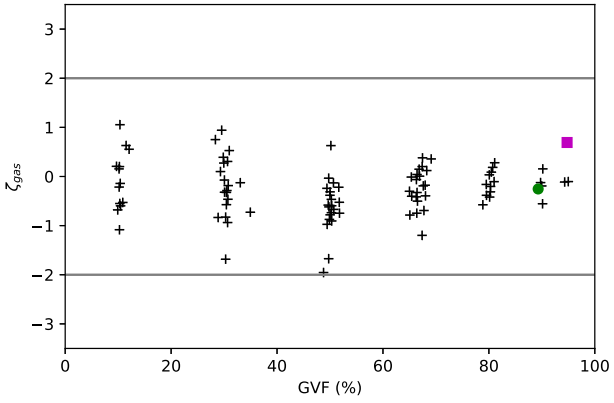

Fig. 5. High pressure ζ_{gas} values presented as a function of GVF.

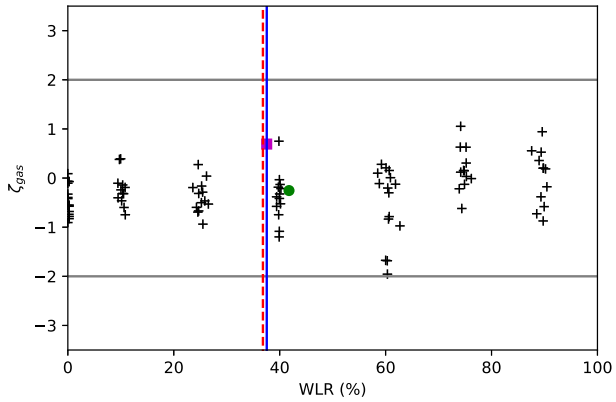

Fig. 6. High pressure ζ_{gas} values presented as a function of WLR.

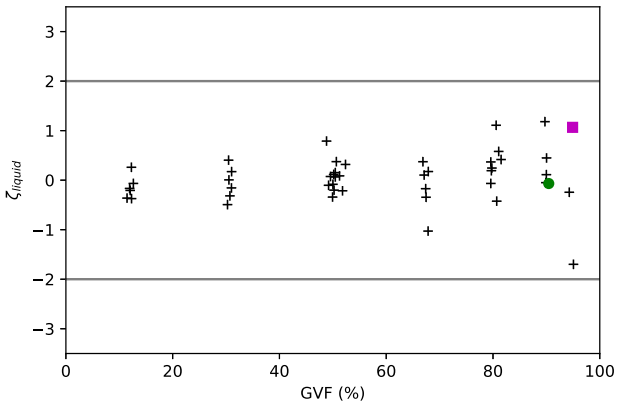

Fig. 7. Low pressure ζ_{liquid} values presented as a function of GVF.

flow. As may have been expected, the majority of points again show strong reproducibility, though this is not the case for the flagged points, TP55 and TP56. The reproducibility of TP56 is calculated as $\zeta_{water} = -4.17$ at low pressure and $\zeta_{water} = -5.35$ at high pressure; therefore, this point is not visible in Figs. 11–14. These values are well outside the threshold for metrological compatibility failure and, although this test point is an isolated anomaly, this may have increased the corresponding U_{repro} values. The reproducibility of TP55 is calculated to be strong in both cases, though the ζ_{water} is noticeably larger at the higher pressure.

Figs. 15–18 present the trends in ζ_{oil}, with respect to GVF and WLR. There are a number of marked differences between these trends and those for ζ_{water}, with several points falling outside the region of metrological compatibility, particularly at higher pressure. Furthermore, there is a distinct decrease in ζ_{oil} at higher WLR values; this is in keeping with the MPFM operating in the water continuous mode.

The results form this section provide important insight into the reproducibility of the transfer package. It can be concluded that it is

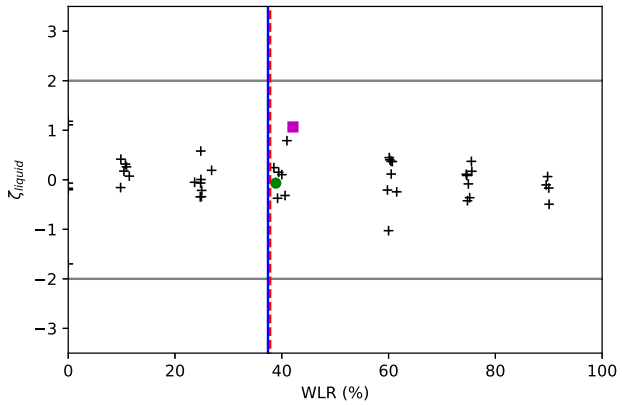

Fig. 8. Low pressure ζ_{liquid} values presented as a function of WLR.

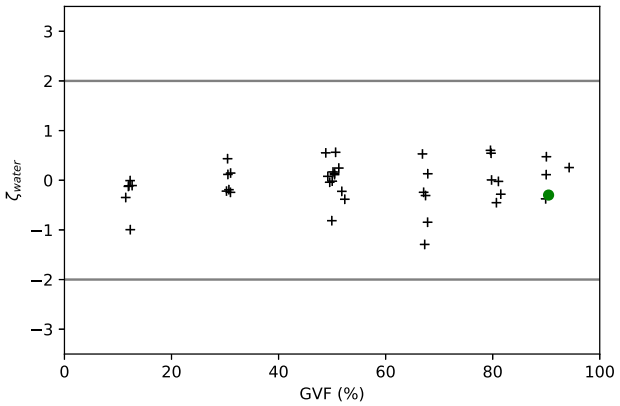

Fig. 11. Low pressure ζ_{water} values presented as a function of GVF.

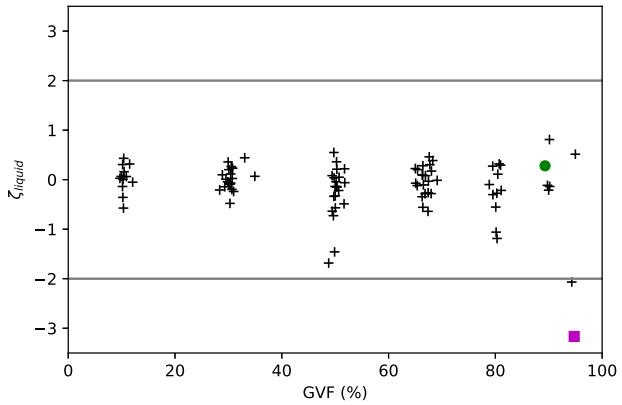

Fig. 9. High pressure ζ_{liquid} values presented as a function of GVF.

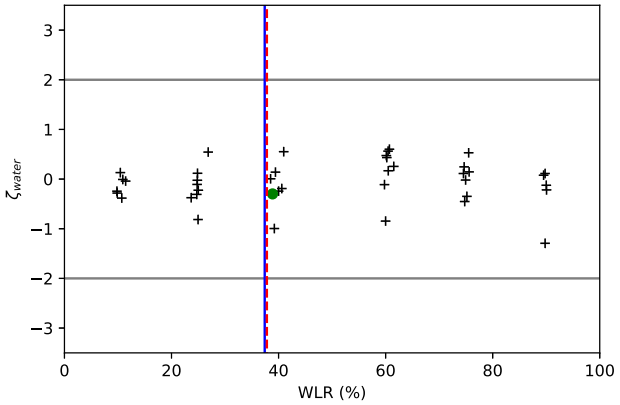

Fig. 12. Low pressure ζ_{water} values presented as a function of WLR.

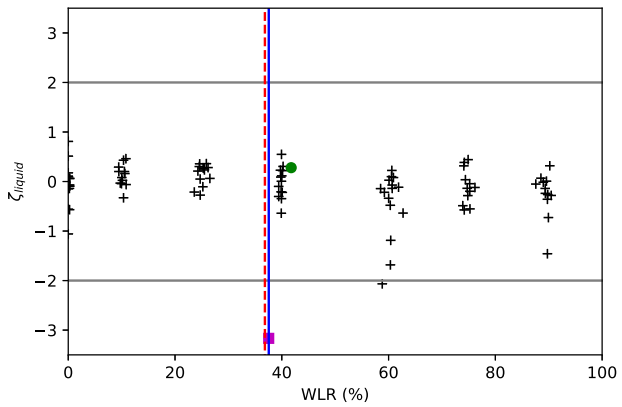

Fig. 10. High pressure ζ_{liquid} values presented as a function of WLR.

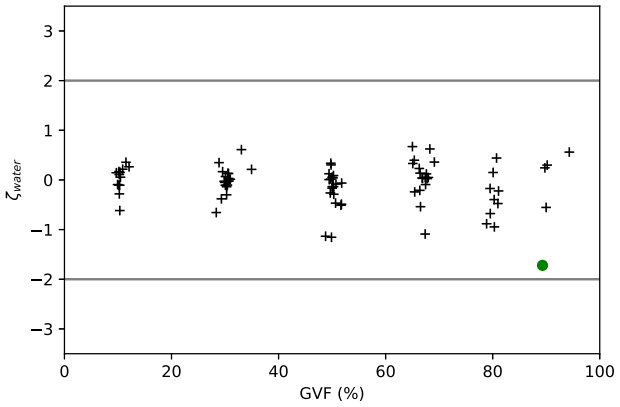

Fig. 13. High pressure ζ_{water} values presented as a function of GVF.

possible to make direct comparisons between laboratories, as will be undertaken in the following section.

5. Inter-laboratory reproducibility

In this section, the ζ parameter is used to investigate the reproducibility between test campaigns undertaken at different laboratories. In light of the conclusions of the previous section, it is unnecessary for these comparisons to be made for both rounds undertaken at NEL, so only the first is used.

Similarly to the previous section, there are two test points, close to the oil/water continuous inversion point, that have been flagged for the comparison between NEL and NORCE. In particular, TP39 and TP41 were recorded as oil continuous at NEL, but water continuous at NORCE. As such, these points have been highlighted in this section with a green circle and magenta square, respectively.

5.1. Q_{gas} comparison

Figs. 19 and 20 present the calculated ζ_{gas} values for the comparison between NEL and NORCE, and the corresponding comparisons for NEL and DNV GL are shown in Figs. 21 and 22. The immediate conclusion from these figures is that the reproducibility is much stronger in the first case. However, it must be noted that there is a marked difference

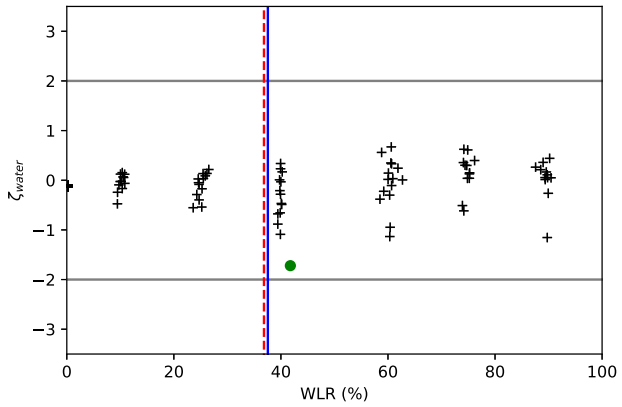

Fig. 14. High pressure ζ_{water} values presented as a function of WLR.

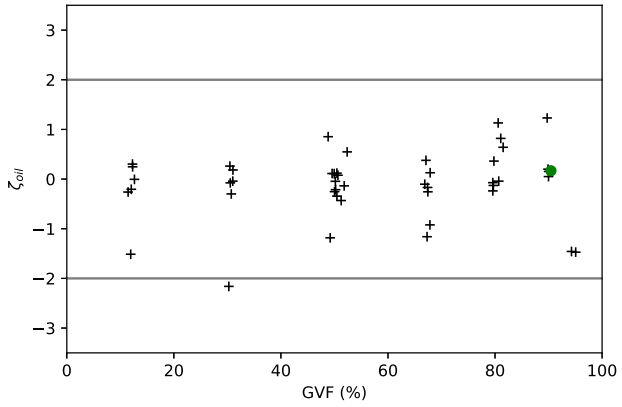

Fig. 15. Low pressure ζ_{oil} values presented as a function of GVF.

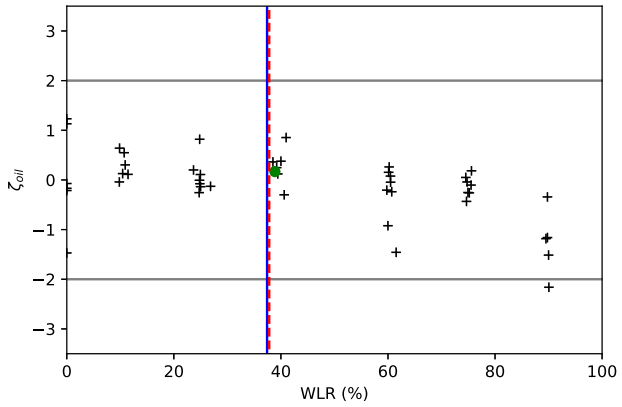

Fig. 16. Low pressure ζ_{oil} values presented as a function of WLR.

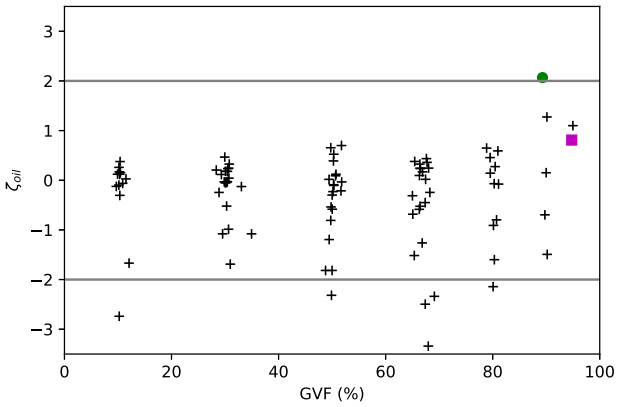

Fig. 17. High pressure ζ_{oil} values presented as a function of GVF.

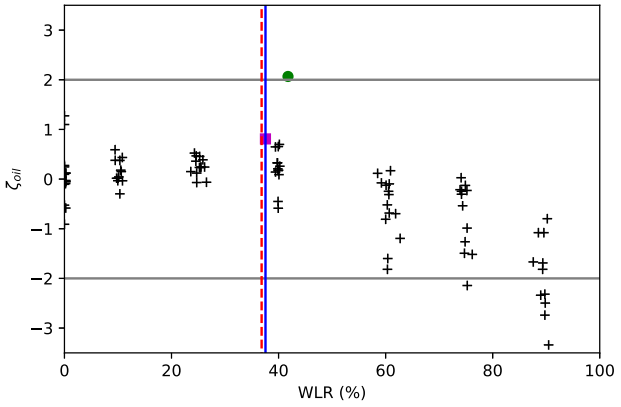

Fig. 18. High pressure ζ_{oil} values presented as a function of WLR.

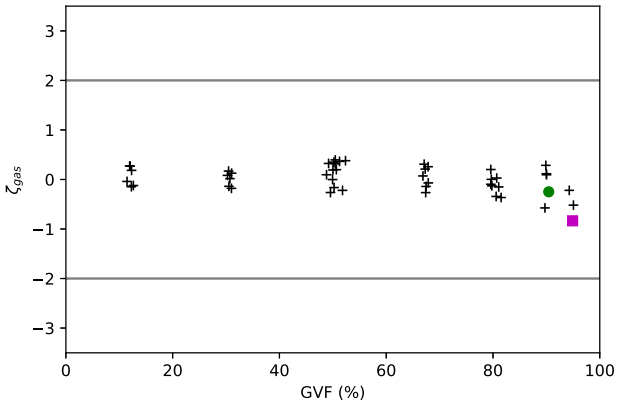

Fig. 19. ζ_{gas} values presented as a function of GVF.

in the calculated uncertainties, as the calculations at NORCE account for the uncertainty of the interphase mass transfer effect.

A result of this difference is that trends in the pairwise comparison are less visible, despite the absolute variations being consistent between the two cases. In particular, Figs. 21 and 22 present a number of test points with low GVFs and WLRs, for which metrological compatibility is not achieved. These variations are believed to caused by phase transitions that occur between the inlet and the transfer package. A more detailed explanation of this phenomenon is beyond the scope of this paper, though would provide an interesting follow-up study.

5.2. Q_{liquid} comparison

As with the ζ_{gas} values, the majority of ζ_{liquid} scores suggest that metrological compatibility has been achieved (Figs. 23–26). In the cases in which $|\zeta_{liquid}| > 2$, these have largely occurred at higher GVFs and lower WLRs. This result may be expected, as absolute deviations will be more pronounced when converted to relative variations.

The low-GVF, low-WLR test points that did not achieve consistency for Q_{gas} were still able to achieve very low ζ_{liquid} values. However, the trends at both pressures levels suggest that it is the high-GVF, low-WLR test points that show the lower levels of reproducibility. In Fig. 26, the greatest variation is observed at the transition from oil continuous

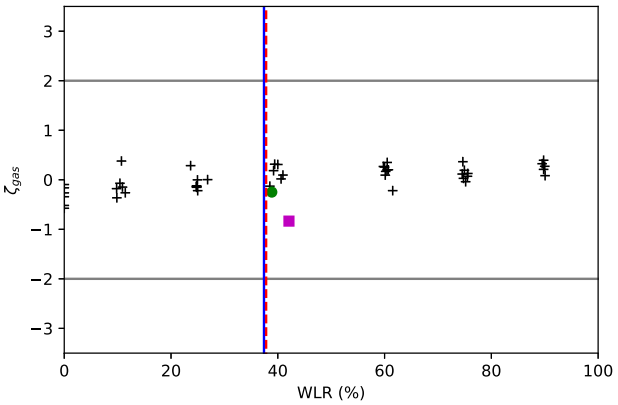

Fig. 20. ζ_{gas} values presented as a function of WLR.

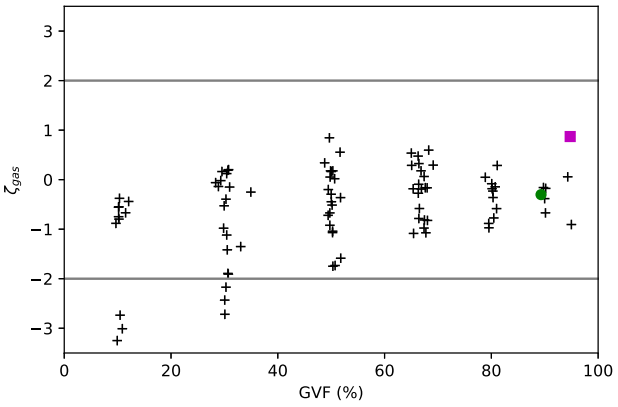

Fig. 21. ζ_{gas} values presented as a function of GVF.

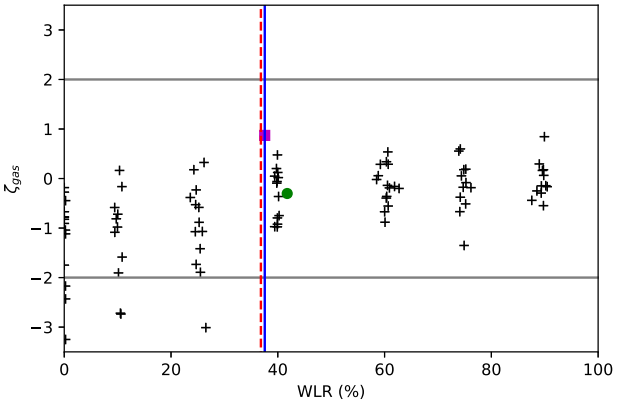

Fig. 22. ζ_{gas} values presented as a function of WLR.

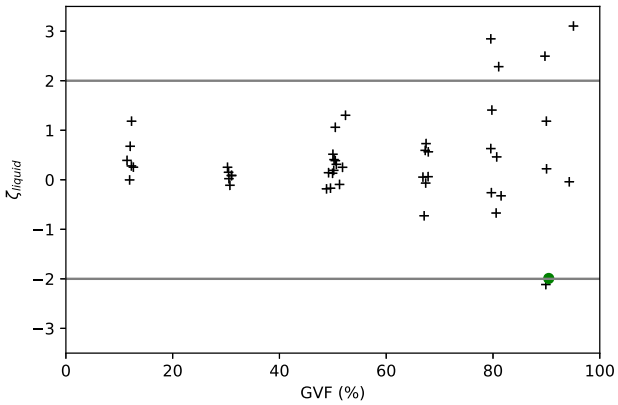

Fig. 23. ζ_{liquid} values presented as a function of GVF.

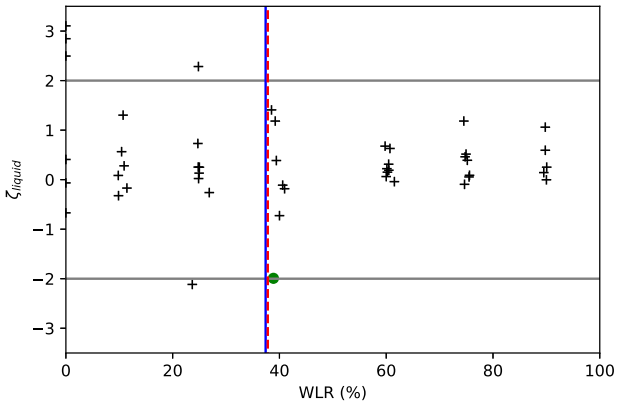

Fig. 24. ζ_{liquid} values presented as a function of WLR.

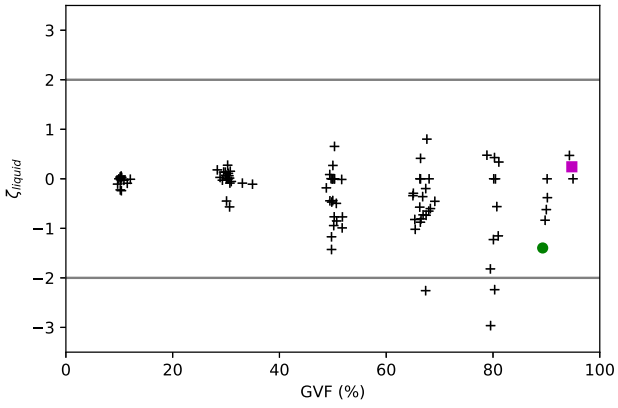

Fig. 25. ζ_{liquid} values presented as a function of GVF.

to water continuous. The MPFM calculates the mode of measurement based on the flow conditions, making this transitional region more complicated to measure.

With regard to the aforementioned flagged points, it can be seen that the reproducibility of TP39 was very low, but that TP41 was considerably beyond the threshold. Despite this, Fig. 23 suggests that this lack of consistency is related more to the GVF, rather than the variations in the MPFM operating mode.

5.3. Q_{water} comparison

The variation in Q_{water} (Figs. 27–30) is also observed to be greatest closest to the oil–water inversion point. This trend is most prominent in Fig. 28. Observing the trend in Fig. 27, it can be concluded that it is the high-GVF points close to this inversion that show the greatest variation. The relatively low ζ_{water} value for TP41 provides further evidence that the inclusion of this test point should not unfairly alter the reproducibility investigation.

As well as the influence of the phase inversion point, high GVFs also appear to contribute to lower reproducibility at both pressure levels. At higher pressures, it can be further observed that high WLRs may also contribute. Although this result may seem counter-intuitive, similar observations were made in the reproducibility tests conducted at NEL.

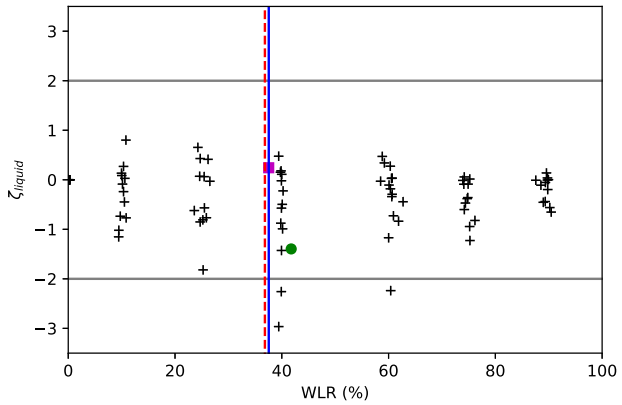

Fig. 26. ζ_{liquid} values presented as a function of WLR.

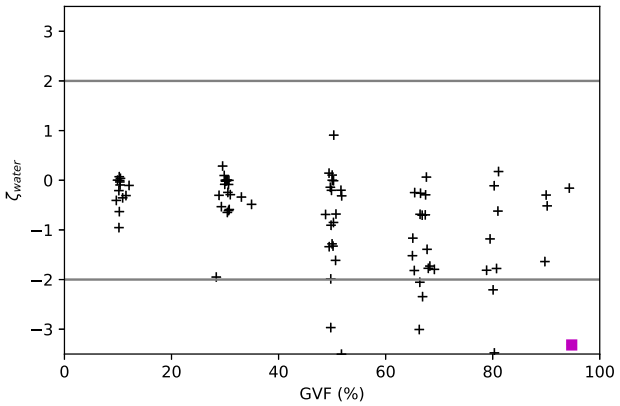

Fig. 29. ζ_{water} values presented as a function of GVF.

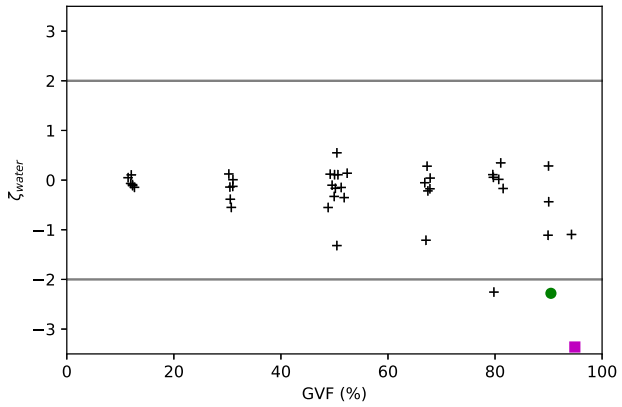

Fig. 27. ζ_{water} values presented as a function of GVF.

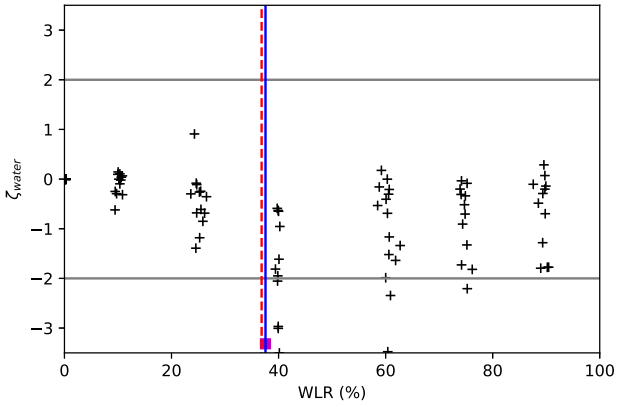

Fig. 30. ζ_{water} values presented as a function of WLR.

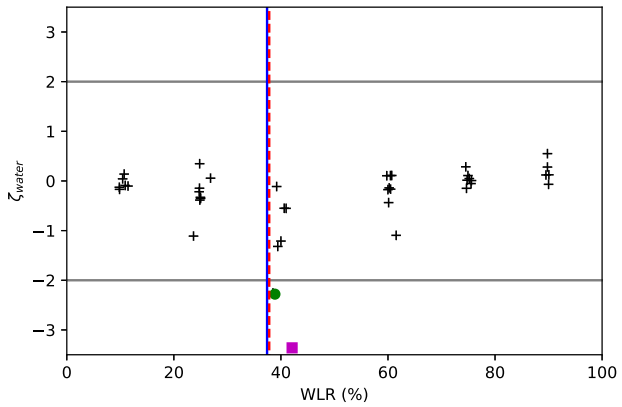

Fig. 28. ζ_{water} values presented as a function of WLR.

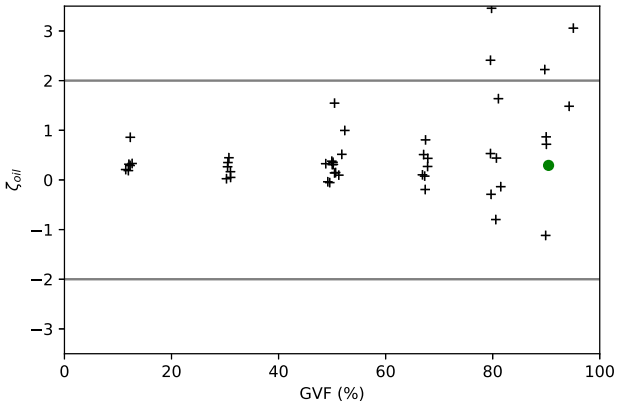

Fig. 31. ζ_{oil} values presented as a function of GVF.

5.4. Q_{oil} comparison

In keeping with the observations made throughout this section, the test points close to the transition point provide the greatest variation in the inter-laboratory comparisons, with lower consistency achieved in the oil continuous region than for water continuous (Figs. 31–34). Here, it can also be seen that high-GVF, low-WLR points also exhibit relatively low reproducibility. Similarly to the discussions regarding ζ_{water}, the observation that ζ_{oil} appears greatest at low WLRs – representing lower reproducibility – seems counter-intuitive. As with discussions of ζ_{gas} variations, further investigations into the explanation for this are beyond the scope of the current project, but could prove to be an interesting follow up study.

6. Conclusions

This paper investigates reproducibility in multiphase flow metrology through analysis of the intercomparison of laboratories undertaken as part of the MultiFlowMet II project. To minimise the influence of laboratory effects on the reproducibility, a standard transfer package and testing protocol was established and implemented across three multiphase flow laboratories. The suitability of each point of the test matrix was calculated using Mandel's h statistic, in accordance with international standard ISO 5275-2:2019, and proved that all points were suitable for intercomparison.

To quantify the reproducibility of the transfer package, a ζ parameter has been established. For a specific test point, repeated either

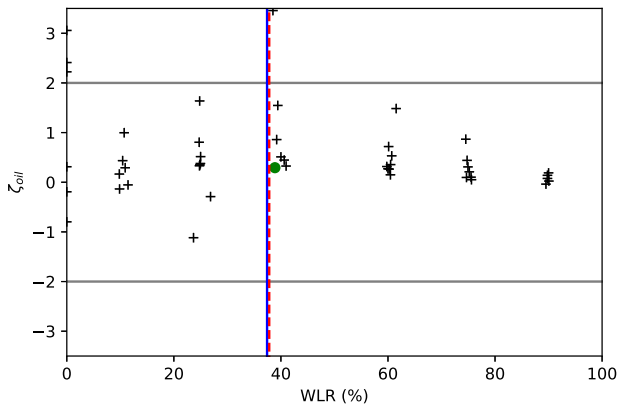

Fig. 32. ζ_{oil} values presented as a function of WLR.

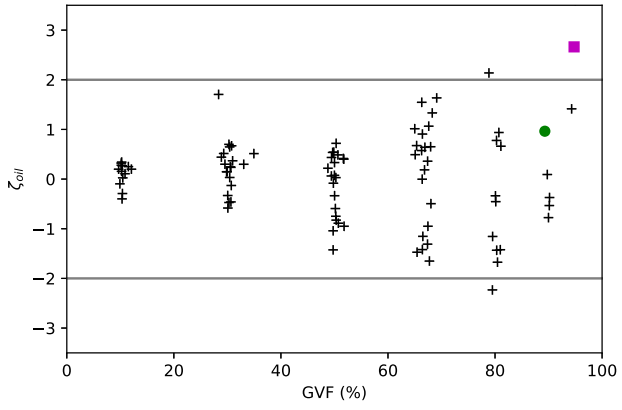

Fig. 33. ζ_{oil} values presented as a function of GVF.

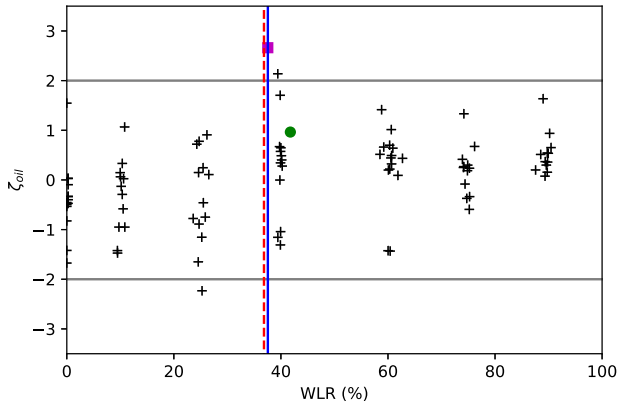

Fig. 34. ζ_{oil} values presented as a function of WLR.

at two laboratories or at different times for the same laboratory, it is claimed that metrological compatibility has been achieved if the ζ value is less than a specified threshold, κ. In this study, a value of $\kappa = 2$ was chosen, so that metrological equivalence is achieved if the relative deviation of the two measurements is less than their combined uncertainty. This parameter has been applied to pairwise comparisons of the test points, both for the repeated tests undertaken at NEL, and the test campaigns at NORCE and DNV GL. A number of important trends have been presented, particularly highlighting the challenges faced for measurements taken in the transitional region between oil and water continuous flow.

Reproducibility uncertainties have been calculated for the transfer package, with all uncertainties less than 10%. It has been shown that, as may be expected, the measurement of liquid flow rates exhibit the smallest level of uncertainty. Once more, there is a noticeable difference between the uncertainties calculated at higher and lower pressures.

They key results for the field of flow metrology can be summarised as follows:

- The reproducibility uncertainties achieved in this intercomparison are comparable with those in the original *MultiFlowMet* project for fluid flow rates, though this was not the case for gas volume flow rates. With the two projects utilising different MPFMs, the insight provided in this work should be considered in the metrology of multiphase flow.
- In the intercomparison between higher-pressure laboratories, variations in the gas reproducibility parameter were observed to be greater for low-GVF, low-WLR test points. As such, it is possible that the uncertainty of measurements for higher GVF and WLR may be lower than those stated here.
- The phase inversion was consistently observed to be an area of low reproducibility, suggesting that extra care and consideration should be applied for measurements taken in such conditions. Knowledge of the phase inversion point for a specific laboratory will provide useful context in these applications.

Funding

This work is funded by the European Metrology Research Programme, UK (ENG58 – MultiFlowMet) project 'Multiphase flow metrology in the Oil and Gas production', and the European Metrology Programme for Innovation and Research, UK (16ENG07 – MultiFlowMet II) project 'Multiphase flow reference metrology', which are jointly funded by the European Commission, UK and participating countries within Euramet and the European union.

CRediT authorship contribution statement

A.J. Elliott: Methodology, Software, Validation, Formal analysis, Data curation, Writing - original draft, Writing - review & editing, Visualization. **G. Falcone:** Conceptualization, Methodology, Investigation, Resources, Writing - review & editing, Supervision, Project administration. **D. van Putten:** Conceptualization, Methodology, Formal analysis, Investigation, Resources, Writing - review & editing. **T. Leonard:** Conceptualization, Methodology, Formal analysis, Investigation, Resources, Writing - review & editing. **K. Haukalid:** Conceptualization, Methodology, Formal analysis, Investigation, Resources, Writing - review & editing. **B. Pinguet:** Conceptualization, Resources, Writing - review & editing.

Declaration of competing interest

The authors declare that they have no known competing financial interests or personal relationships that could have appeared to influence the work reported in this paper.

References

[1] Publishable Summary for 16ENG07 – MultiFlowMet II Multiphase flow reference metrology, EURAMET (2018).
[2] ENG 58 final publishable JRP report and associated annex A, EURAMET (2018).
[3] G. Kok, D. van Putten, L. Zakharov, Results from an intercomparison between multiphase flow test facilities, in: Proceedings of FLOMEKO 2019, Lisbon, Portugal, 2019.
[4] Bryce M. Hand, Supercritical flow in density currents, J. Sediment. Res. 44 (1974).
[5] International Organization for Standardization, Accuracy (Trueness and Precision) of Measurement Methods and Results – Part 2: Basic Method for the Determination of Repeatability and Reproducibility of a Standard Measurement Method (ISO 5725-2:2019), vol. 2019, Standard, Geneva, Switzerland, 2019.

[6] J. Mandel, A new analysis of interlaboratory test results, in: Proceedings of the 39th Annual Quality Congress, May 1985, Maltimore, MD, vol. 39, 1985, pp. 360–366.
[7] P.-T. Wilrich, Critical values of Mandel's h and k, the Grubbs and the Cochran test statistic, 97 (2013) 1–10.
[8] International Organization for Standardization, Statistical Methods for Use in Proficiency Testing by Interlaboratory Comparison (ISO 13528:2015), vol. 2015, Standard, Geneva, Switzerland, 2015.
[9] Rüdiger Kessel, Raghu N. Kacker, Klaus-Dieter Sommer, Combining results from multiple evaluations of the same measurand, J. Res. Natl. Inst. Stand. Technol. 116 (2011) 809–820.